Modeling of drug release, erosion and diffusion fronts movement in high viscosity HPMC matrices containing a cellulolytic enzyme

Ilaria Filippin[1], Saliha Moutaharrik[1]*, Michela Abrami[2], Lucia Grassi[2], Andrea Gazzaniga[1], Alessandra Maroni[1], Mario Grassi[2], Anastasia Foppoli[1]

[1]Università degli Studi di Milano
Dipartimento di Scienze Farmaceutiche
Sezione di Tecnologia e Legislazione Farmaceutiche "Maria Edvige Sangalli"
via G. Colombo 71
20133 Milano, Italy

[2]Università degli Studi di Trieste,
Dipartimento di Ingegneria e Architettura
Building B, via Valerio 6
34127 Trieste, Italy

Corresponding Author:
Saliha Moutaharrik
tel +39 02 50324655
email: saliha.moutaharrik@unimi.it

ABSTRACT

A formerly developed mathematical model describing drug release from hydrophilic matrices (HMs) took into account resistance to drug release given by its dissolution and by the presence of a growing gel layer. Such a model was applied to previously reported release data obtained from HMs made of hydroxypropyl methylcellulose (HPMC), where acetaminophen was used as model drug and a cellulolytic product was added as "active" excipient to attain zero-order release kinetics.

The Levich theory applied to acetaminophen IDR data highlighted the suitability of such a drug for modeling purposes, given its good surface wettability. First assessment of the model ability to describe drug release from the abovementioned systems was carried out on partially coated matrices, representing a simplified physical frame, but results were then confirmed on uncoated systems. Experimental and model release data showed good agreement; therefore, the release-describing equation was combined with that of the global mass balance to obtain two new equations related to erosion and diffusion fronts time evolution. Changes over time in the dissolution and gel contributions to total resistance, calculated using model output parameters, highlighted that the enzyme, through its hydrolytic activity on HPMC, was responsible for a time-dependent reduction of the resistance component related to gel layer.

KEYWORDS

Mathematical Modeling

Hydroxypropylmethylcellulose (HPMC)

Hydrophilic matrix

Cellulase

Erosion and swelling fronts

Release mechanism

1. INTRODUCTION

Prolonged-release systems are designed to maintain the therapeutic effect of a selected drug for an extended period of time (Wang et al., 2020). This feature generally avoids the peak-valley plasmatic concentration profile typical of multiple administrations of conventional release dosage forms, thus possibly lowering the probability of side effects occurrence and reducing the number of administrations, ultimately improving patients' compliance (Jantzen and Robinson, 2002).

Hydrophilic matrices (HMs) are well-established prolonged release dosage forms (Ghori and Conway, 2015). They are robust systems which show poor manufacturing complexity, as they are generally obtained from consolidated techniques such as tableting, casting or extrusion of a drug – swellable polymer mixture (Loreti et al., 2013; Wen et al., 2010; Zhang and McGinity, 1999). The hydrophilic derivatives of cellulose, particularly hydroxypropyl methylcellulose (HMPC), are the most frequently utilized class of swellable polymers for the preparation of HMs.

As all prolonged release systems, HMs are in principle designed to provide zero-order kinetics, a prerequisite to achieve constant plasma drug levels throughout the whole release duration (Laracuente et al., 2020). Nevertheless, upon contact with the aqueous media, matrices are subjected to various and concomitant phenomena which result in a non-linear release profile (Colombo, 1993; Timmins et al., 2016; Tiwari et al., 2011; Vázquez et al., 1992). After a burst effect due to drug dissolution at the matrices surface, a pseudo-linear phase can be observed. In this segment, the polymer undergoes a glass-rubbery transition with the formation of a gel layer (Jamzad et al., 2005). The drug, which dissolves at the swelling front (*i.e.* the surface between the matrix still in the glassy state and the gel layer) can diffuse through the gel to reach the outer surface of the matrix (*i.e.* erosion front) and finally be liberated into the dissolution medium (Colombo et al., 2000, 1987; Tiwari and Rajabi-Siahboomi, 2008). A third front delimiting a gel layer area with undissolved drug, namely diffusion front, can be present. Its position

depends on drug solubility and drug load (Colombo et al., 1999; Ferrero et al., 2010). The swelling front upon solvent penetration moves inwards, while the erosion front tends to move outwards - because of polymer swelling - until matrix volume increasing is counterbalanced by the polymer erosion-dissolution phenomenon (Deering et al., 2008; Mašková et al., 2020; Salsa et al., 2008). This combined movement is responsible for an increase of drug diffusional path and a decrease of the area available for drug dissolution over time, leading to a progressive drop of drug release rate (Colombo et al., 1995; Harland et al., 1988).

Through the years, many researchers have explored various strategies to obtain zero-order kinetics from HMs, mainly by modifying their basic design in terms of geometry and/or composition. (Cerea et al., 2020a, 2020b, 2018; Conte et al., 1993; Ford et al., 1987; Gander et al., 1988; Gazzaniga et al., 1993; Kim, 1995; Moodley et al., 2011; Ranga Rao et al., 1988; Sangalli et al., 1994). Recently, the use of cellulase, a cellulolytic enzymatic complex, as “active” excipient was proposed in HPMC-based oral delivery systems, namely in a time-dependent reservoir system and in prolonged release HMs (Foppoli et al., 2020; Gazzaniga et al., 2022, Palugan et al., 2021). Cellulase is indeed able to exert hydrolytic activity not only on its natural substrate, cellulose, but also on hydrophilic cellulose derivatives, such as HPMC (Caceres et al., 2020).

As far as matrices are concerned, the observed general increase of release rate was effective in counteracting its late decrease and, when considering relatively high concentration of the enzymatic complex, also in masking the initial burst effect. In depth studies of the mechanisms involved into the release profiles shift towards linearity highlighted that the main phenomena involved in drug release were modified by the hydrolytic action of the enzyme on the polymer, although to a different extent. Specifically, polymer swelling, intended as glassy-rubbery transition rate, was poorly affected by cellulase activity, while erosion and dissolution of the matrices were clearly enhanced because of the formation of shorter polymeric chains (Palugan et al., 2021). In fact, the enzyme-related glycosidic bonds cleavage can be considered as a further phenomenon operating

during drug release, which was also responsible for a faster drug diffusion through an increasingly permeable gel layer. In other words, cellulase could be considered as an “active” excipient which, through its hydrolytic activity, was found able to progressively lower the gel layer resistance to molecular diffusion.

Mathematical modelling of drug release from HPMC matrices has been pursued by many researchers over the years (Peppas and Narasimhan, 2014). In a model previously reported by some of us, the general equation for drug dissolution was adapted to describe drug release from HMs by adding the resistance to drug diffusion, which depends by both contribution of the dissolution phenomenon and the gel layer (Grassi et al., 2004).

In the present work, the suitability of this mathematical model to describe drug release from matrices containing a cellulolytic product was evaluated, and derived new equations able to define the erosion and diffusion fronts positions over time were sought. For a first assessment of the model suitability, previously published data obtained from tableted HMs partially coated on all the surface except for one base were used (Palugan et al., 2021). This feature, allowing the surface of the active substance in contact with the solvent to remain constant, made the physical frame to be modeled less complex. The ability of the equations to predict both release and fronts positions was estimated not only on this simplified configuration, but also on uncoated matrices exposing their entire surface to the dissolution medium.

1.1. Mathematical Modeling

1.1.1. Release and fronts position

Mathematical modeling of drug release from HPMC matrices has attracted the attention of many researchers over the years leading to the publication of various and powerful descriptive models (Adrover et al., 2018; Caccavo et al., 2017;

Chirico et al., 2007; Guiastrennec et al., 2017; Saeidipour et al., 2017; Siepmann and Peppas, 2012, 2001). With the aim to develop a simple and reliable model to describe the behaviuor of HPMC matrices formulated with a cellulolytic enzymatic complex, in this work an already existing mathematical model, which proved to be reliable in describing the release of diprophylline and theophylline from HPMC matrices, was implemented (Grassi et al., 2004). This model was obtained following the main idea of generalizing the classical Noyes and Whitney (Noyes and Whitney, 1897) equation describing the dissolution of drug particles (Siepmann and Siepmann, 2013):

$$\frac{dC}{dt} = \frac{D\,A}{V\,h}(C_s - C) \qquad (1)$$

where t is time, C and C_s are drug concentration and solubility in the dissolution medium, respectively, D is the diffusion coefficient in the dissolution medium, A is the surface area at the solid/liquid interface, V is the dissolution medium volume, h is the stagnant layer thickness surrounding the solid and the ratio D/h represents the intrinsic dissolution rate constant k_d. Obviously, eq.(1) holds in the hypothesis of negligible mass transport resistance at the solid-liquid interface, this being typical of easily wettable solids (Abrami et al., 2020). Bearing in mind that the global diffusional resistance of a multi-layered membrane is the sum of the resistance of each layer (Flynn et al., 1974), eq.(1) can be adapted to describe drug release from a hydrophilic matrix by properly incorporating the diffusion step of the drug through the gel layer:

$$\frac{dC}{dt} = \frac{\varphi_d\,A}{V}\frac{(C_s - C)}{\left(\frac{1}{k_d} + R\right)} \qquad (2)$$

where j_d is the drug volume fraction and R the gel layer resistance ($1/R$ can also be defined as gel permeability, P). The global resistance to drug release is given by the sum of the dissolution phenomenon resistance ($1/k_d$) and the resistance to

drug diffusion through the gel layer (R). As A represents the area at the interface between the polymer in the glassy and rubbery state (*i.e.* at the swelling front), $j_d A$ indicates the drug-liquid surface area at the swelling front (Lombardi et al., 1998). Notably, eq.(2) also holds for drug release in non-sink conditions due to the presence of the (C_s - C) term and it has the advantage of degenerating into eq.(1) for tablets made of drug only (j_d = 1; R = 0). As drug diffusion rate through a gel layer can reasonably be correlated to the layer thickness, the analysis of experimental data regarding the temporary evolution of the gel thickness (Cappello et al., 1994; Colombo et al., 1999; Sai Cheong Wan et al., 1995) leads to conclude that a reasonable, although empirical, R time variation can be expressed by eq.(3):

$$R = B(1\text{-}e^{-bt}) \tag{3}$$

where B represents the asymptotic value of R and b rules the kinetics of R variation. Both B and b are model parameters to be determined by data fitting.

Due to its empirical nature, equation (3) can properly account for other phenomena concurring to the diffusional resistance such as the influence of variation of A over time and the drug transport in different directions. When dealing with cylindrical tablets that are coated on all the surface except one base with an impermeable film, A is substantially constant and drug transport is, essentially, one-dimensional (the direction normal to the tablet plane surface). On the contrary, in the case of uncoated tablets, A is time dependent and drug diffusion becomes, in principle, three-dimensional.

Embodying eq.(3) into eq.(2) and solving for C assuming that drug concentration (C) in the release environment is zero at the beginning of the experiment (t = 0), leads to model analytical expression (Demidovic, 1975) of eq.(4):

$$C = C_s\left(1 - \left(e^{bt}\left(1 + Bk_d(1 - e^{-bt})\right)\right)^{-\frac{A\varphi_d}{bV\left(B+\frac{1}{k_d}\right)}}\right) \tag{4}$$

which, in terms of amount of drug released ($M = CV$) becomes eq.(5):

$$M = VC_s\left(1 - \left(e^{bt}\left(1 + Bk_d(1 - e^{-bt})\right)\right)^{-\frac{A\varphi_d}{bV\left(B+\frac{1}{k_d}\right)}}\right) \quad (5)$$

It should be noted that eq.(4) or (5) hold as far as either drug solid particles and a glassy portion of the matrix exist, *i.e.* until the swelling front reaches the bottom of the coated tablet or the center of the uncoated one.

Interestingly, coupling of eq.(4) with the global drug mass balance enables the theoretical evaluation of the time position of both the dissolution (Xd) and the erosion (Xe) fronts. Indeed, the global mass balance ensures that the initial drug amount contained in the tablet (M_0) must be equal, at any time, to the amount of drug released in the medium ($C \cdot V$) plus the amount still present in the tablet ($A \cdot X_d \cdot C_0 + M_g$), according to eq.(6):

$$M_0 = CV + AX_dC_0 + M_g \quad (6)$$

where C_0 is the initial drug concentration in the tablet and M_g is the drug amount contained inside the gel layer. Assuming a linear decrease of drug concentration within the gel layer, *i.e.* from the diffusion to the erosion front (Figure 1), M_g can be estimated according to eq.(7):

$$M_g = A\int_0^{X_e - X_d}\left(\frac{C - C_s}{X_e - X_d}y + C_s\right)dy = A(X_e - X_d)\left(\frac{C + C_s}{2}\right) \quad (7)$$

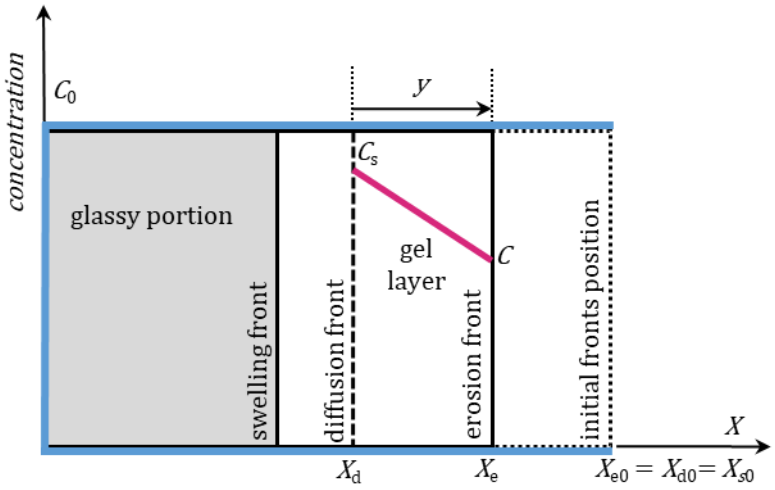

Figure 1. Schematic of fronts position and drug concentration profile in a partially coated hydrophilic matrix. C_0, C_s and C represent, respectively, the initial drug concentration in the tablet, the drug solubility and the drug concentration in the external fluid. X_e, X_d and X_s indicate, respectively, the erosion, the diffusion and the swelling fronts positions while X_{e0}, X_{d0} and X_{s0} are the respective positions at t=0.

Remembering that R represents the mass transfer resistance inside the gel layer, its mathematical definition reads:

$$R = \frac{X_e - X_d}{D_m k_p} \tag{8}$$

i.e., R is the ratio between the gel layer thickness ($X_e - X_d$) and the product of drug diffusivity in the gel (D_m) times the drug partition coefficient (k_p) between the gel and the external liquid phase. Should the diffusing drug molecules interact with the polymer chains and/or should the gel structure not be homogeneous, D_m can be considered as an effective diffusion coefficient, the values of which depends on the strength of drug interaction with polymeric chains and the gel structure heterogeneity (Grassi et al., 2006). Eq.(8) allows expressing the gel layer thickness ($X_e - X_d$) as the product $R \cdot D_m \cdot k_p$ that, in turn, can be embodied into eq.(6) in order to easily determine X_d:

$$X_d = \frac{M_0}{AC_0} - \frac{\left(\frac{V}{A}+\frac{RD_m k_p}{2}\right)+RD_m k_p \frac{C_S}{2}}{C_o} \quad (9)$$

Finally, in the light of eq.(8), it is possible getting the position of the erosion front X_e:

$$X_e = \frac{M_0}{AC_0} - \frac{C\frac{V}{A}+RD_m k_p\left(\frac{C+C_S}{2}-C_o\right)}{C_0} \quad (10)$$

It is important to underline that at the beginning of the experiment (t = 0), both R and C are equal to zero, so that the positions of the erosion and the diffusion front coincide, residing in the initial surface of the tablet in contact with the fluid. In addition, coherently, subtraction of eq.(9) from eq.(10) provides the gel layer thickness ($X_e - X_d$) that, according to eq.(8) is equal to $R \cdot D_m \cdot k_p$.

In conclusion, the proposed model is characterized by four fitting parameters. B and b connected to the evolution of the gel layer thickness (eq.(3)), k_d related to the intrinsic drug dissolution (eq.(2)) and D_m that is the average drug diffusion coefficient in the gel layer (eq.(8)). The simultaneous fitting of eq.(5) and eq.(10), respectively, to the experimental data referring to the amount of drug released and the position of the erosion front, allows the determination of B, b, k_d and D_m.

1.1.2. Intrinsic Dissolution Rate (IDR)

To better understand the physics of drug release from HPMC matrices containing different amounts of cellulase, it is useful to theoretically analyze the outcomes of intrinsic dissolution rate (IDR) test (Grassi et al., 2006). Fixed or rotating disk configurations are typically the most common apparatuses used to perform IDR tests. In the former configuration, which was selected for this work, the relative velocity between the stationary disk and the fluid under motion (given by the paddle rotating at different speed) affects the rate of drug dissolution, the kinetics of which is essentially regulated by the formation of a stagnant liquid layer adjacent to the solid surface.

The simultaneous solution of the momentum and the continuity equations referred to the dissolution medium and the solution of the mass balance equation referred to the drug, allowed Levich (Levich, 1962) to demonstrate that, in the rotating disk configuration, the average stagnant layer thickness δ, is given by:

$$\delta = 1.61 \sqrt[3]{\frac{D}{\nu}} \sqrt{\frac{\nu}{\omega}} \tag{11}$$

where ν is the dissolution medium kinematic viscosity and D is the drug diffusion coefficient in the dissolution medium and ω is the angular velocity of the fluid-disk relative motion. A similar analysis led by Khoury and co-workers (Khoury et al., 1988) on the fixed disk configuration, revealed that eq.(11), basically, still holds but with a different multiplying constant, to be determined from experimental data. Consequently, the intrinsic dissolution constant k_d, *i.e.* the ratio between D and δ, descending from the Levich approach (eq.(11)) still holds but with a different multiplying constant ($F_a \cdot 0.621$):

$$k_d = \frac{D}{\delta} = F_a 0.621 D^{\frac{2}{3}} \nu^{-\frac{1}{6}} \sqrt{\omega} \tag{12}$$

In the IDR case, eq.(2) becomes (Abrami et al., 2020):

$$\frac{dC}{dt} = \frac{S}{V} \frac{(C_s - C)}{\left(\frac{1}{k_d} + \frac{1}{km}\right)} \tag{13}$$

where S is the dissolution area, V is the dissolution medium volume and k_m is the interface mass transfer coefficient mainly depending on the dissolution surface wettability. In other words, $1/k_d$ and $1/k_m$ represent, respectively, mass transfer resistance due to the presence of the stagnant layer and due to solid surface wettability issues. Eq.(13) solution, in the light of eq.(12), leads to eq.(14):

$$C = C_s\left(1 - e^{\left(-\frac{S}{V}\frac{t}{\frac{1.61}{F_a}D^{-\frac{2}{3}}\nu^{\frac{1}{6}}\omega^{-\frac{1}{2}}+\frac{1}{k_m}}\right)}\right) \quad (14)$$

where F_a and k_m need to be determined by eq.(14) fitting to experimental IDR data performed at different paddle rotation speed.

2. EXPERIMENTAL

2.1. Materials

Acetaminophen (AMP, C.F.M., Italy), M_w 151,2 g/mol, water solubility 18 g/L at 37 °C, true density 1.214 g/cm^3. Hydroxypropyl methylcellulose 2208 USP (HPMC, Methocel® K4M, Mn = 86000, Dow Italia, Italy), true density 1.326 g/cm^3. Sternzym® C13030 (SternEnzym GmbH and Co. KG, Germany -kindly donated by IMCD Italia, Italy) 2500 U/g enzymatic activity, expressed as hemicellulase according to DNS method at pH 6.0 as reported in the product technical data sheet. Cellulose acetate propionate (CAP 482–20, Eastman-Kodak, Tennessee, US).

2.2. Methods

2.2.1. Intrinsic dissolution test

AMP powder samples were compacted by means of a hydraulic press in a round Ø=11 mm matrix, under approximately 3 tons force for 3 min. The obtained compacts were maintained inside the matrix and tested in a USP43 Apparatus 2 (Distek Dissolution System 2100B) under the following conditions: 500 mL of distilled water at 37°, paddle height set at 2.5 cm from the compacts surface, rotation speed 50, 75, 100 or 125 rpm. The concentration of drug in the dissolution medium at each time point was determined spectrophotometrically at 243 nm. The test was performed in 3 replicates.

2.2.2. True density determination

Literature-reported true density values were used for AMP (1.214 g/cm^3) and HPMC (1.326 g/cm^3) (ECHA, 2012; Rogers T L, 2009). For the cellulolytic product, the value was experimentally determined. Sternzym® C13030 powder was compacted in a round Ø=11 mm matrix with a hydraulic press applying 15 tons force for 6 min under vacuum (n=3). Then, weight and height of each compact were measured to calculate true density (1.391 g/cm^3).

2.2.3. Preparation and testing of matrices

Mass loss, release, erosion and swelling fronts positions data used for mathematical modeling are those published in Palugan et al., 2021. Two types of systems were prepared from a mixture of AMP and HPMC in a 1:1 w/w ratio, either as such or containing different amounts of Sternzym® C13030, following the compositions reported in Table 1. Cylindrical flat faced units (diameter 25 mm, height 3.15 mm, nominal weight 1.5 g) were partially coated on the entire surface except for one base with an impermeable film manually applied by dipping into a 15% w/v CAP solution in acetone. The partially coated matrices (CM systems), after being ballasted by gluing the coated base to a stainless-steel disk, were tested for release (spectrophotometric determination of AMP at λ = 243 nm), mass loss by gravimetric method, erosion and swelling fronts position measurements by means of a penetrometer. Uncoated convex-faced units (diameter 11 mm, height 2.2 mm, nominal weight 0.24 g) underwent only release tests (UM systems).

Table 1 – Weight percentage composition of the partially coated (CM) and uncoated matrices (UM) under investigation. Percentage of Sternzym® C13030 is also reported as calculated on HPMC.

Code		AMP	HPMC	Sternzym® C13030	*Sternzym® C13030 wth respect to HPMC*
25 mm partially coated	11 mm uncoated				
CM_0	UM_0	50.00	50.00	-	-
$CM_{0.5}$	$UM_{0.5}$	49.88	49.88	0.25	*0.5*

CM_1	UM_1	49.75	49.75	0.50	*1*
CM_5	UM_5	48.78	48.78	2.44	*5*
CM_{10}	UM_{10}	47.62	47.62	4.76	*10*

3. RESULTS AND DISCUSSION

3.1. IDR

Due to eq.(14) mathematical features, the determination of the unknown parameters F_a and k_m requires the simultaneous fitting of eq.(14) to each set of experimental data, obtained from IDR tests performed at different paddle rotation speed, *i.e.* 50, 75, 100 and 125 rpm (angular velocity ω = (50, 75, 100 and 125 rpm)*π/30)

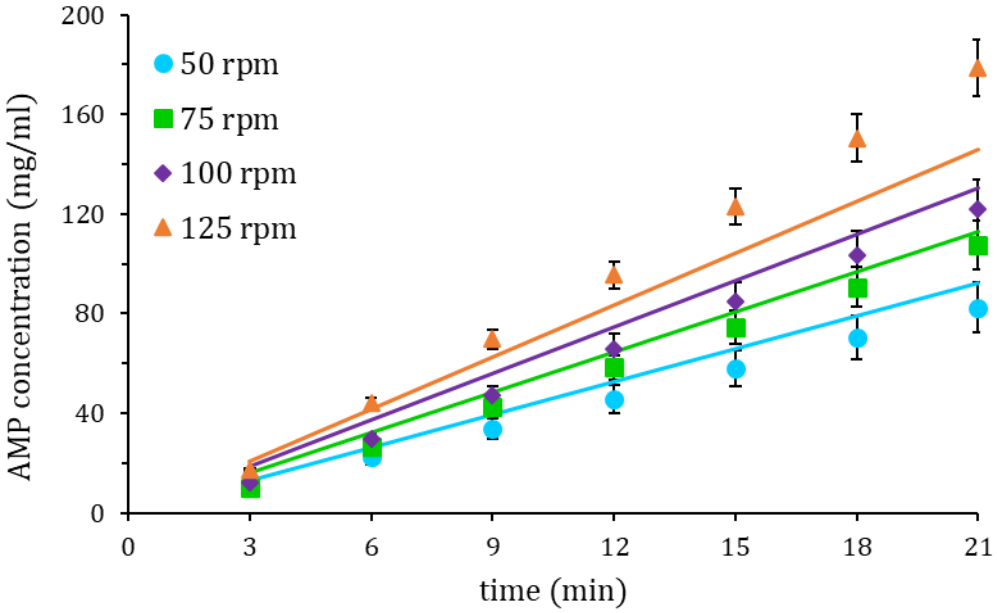

Figure 2. IDR of acetaminophen obtained in thermostated water (T = 37°C) at different paddle rotation speed. Symbols indicate experimental data while lines represent best fitting according to eq.(14). Vertical bars indicate standard deviation

A rather good agreement was found between eq.(14) best fitting and the experimental data corresponding to all the considered paddle velocities (Figure 2). This qualitative statement is statistically supported by the *F*-test score ($F(1, 28, 0.95) < 293$). Data fitting, performed assuming $T = 37°C$, $\nu = 6.96 \cdot 10^{-7}$ m^2/s (water), $C_s = 18$ kg/m^3, $S = 3.8 \cdot 10^{-4}$ m^2 and $V = 5 \cdot 10^{-4}$ m^3 and $D = 7.8 \cdot 10^{-10}$ m^2/s (calculated on the basis of the Stokes-Einstein equation assuming acetaminophen molar volume equal to $1.844 \cdot 10^{-4}$ m^3/mole (Iqbal and Malik, 2005), this corresponding to a radius of 0.418 nm), provides $F_a = (0.42 \pm 0.02)$ and $k_m \geq 1$ m/s as whatever $k_m \geq 1$, fitting quality no longer improves. Notably, the high k_m value ensures that acetaminophen dissolution is substantially not affected by surface resistance to drug dissolution. Indeed, wherever the mass transfer resistance due to interface ($R_m = k_m^{-1}$) is ≤ 1 s/m, the mass transfer resistance due to presence of the stagnant layer ($R_d = k_d^{-1}$) is about five order of magnitude bigger (see Table 2), this meaning that the effect of the stagnant layer on the mass transport is much more important than that exerted by the surface resistance to dissolution. Thus, acetaminophen is easily wettable by water.

Table 2. Model parameters related to eq.(14) fitting to experimental IDR data performed at different paddle rotation speed: interface mass transfer coefficient (k_m), intrinsic dissolution constant (k_d), interfacial (R_m) and hydrodynamic (R_d) mass transfer resistances and thickness (δ) of the stagnant layer adhering to the fixed solid surface. k_m and F_a derive from fitting of eq.(14) to experimental data, δ and k_d are calculated according to eq.(12).

Paddle rotation speed (rpm)	**50**	**75**	**100**	**125**
$\boldsymbol{F_a}$	0.42 ± 0.02			
$\boldsymbol{k_m}$ (m/s)	≥ 1			
$\boldsymbol{k_d}$ (m/s)	$(5.38 \pm 0.25) \cdot 10^{-6}$	$(6.58 \pm 0.3) \cdot 10^{-6}$	$(7.60 \pm 0.36) \cdot 10^{-6}$	$(8.50 \pm 0.40) \cdot 10^{-6}$
$\boldsymbol{R_m}$ (s/m)	≤ 1			
$\boldsymbol{R_d}$ (s/m)	$(1.86 \pm 0.89) \cdot 10^5$	$(1.52 \pm 0.72) \cdot 10^5$	$(1.31 \pm 0.62) \cdot 10^5$	$(1.17 \pm 0.56) \cdot 10^5$
δ (μm)	145 ± 7	118 ± 6	102 ± 5	92 ± 4

3.2. Partially coated matrices

Figure 3 shows the simultaneous best fitting of the proposed mathematical model (lines) to experimental data (symbols) referring to the amount of released acetaminophen (Figure 3A – eq.(5)) and the position of the erosion front (Figure 3B – eq.(10)) relative to the enzyme-free system CM_0. While the statistical reliability of model best fitting is proved by the *F*-test score ($F(3, 19, 09.95) < 9660$), its physical soundness is proved by the values of the fitting parameters. Indeed, k_d ($(4.8 \pm 0.2)*10^{-6}$ m/s) is slightly smaller than $k_{d\text{-IDR}}$ (Table 2). This difference is reasonable, considering that the HPMC network creates an almost static hydrodynamic condition around the particles.

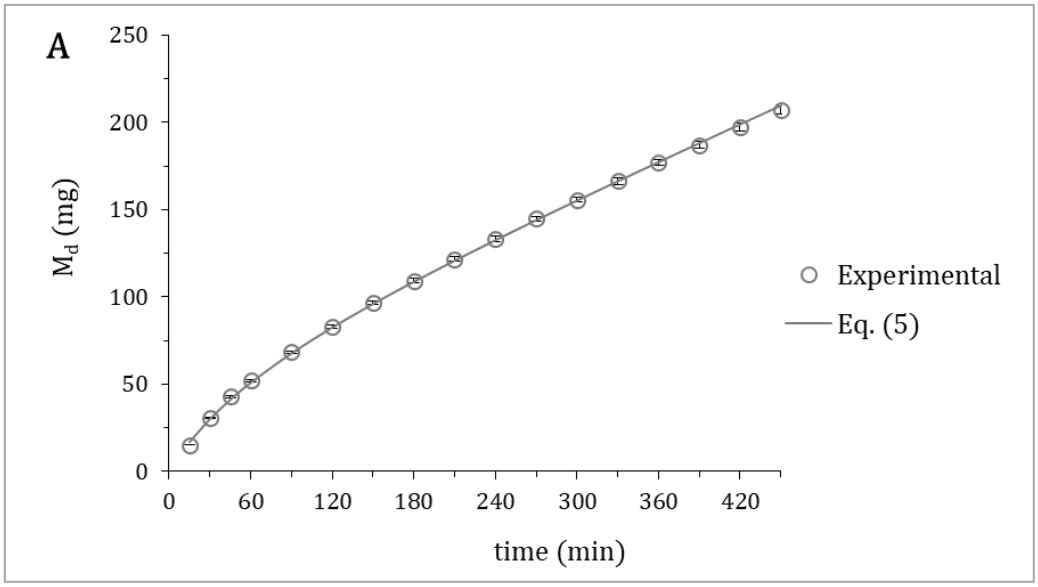

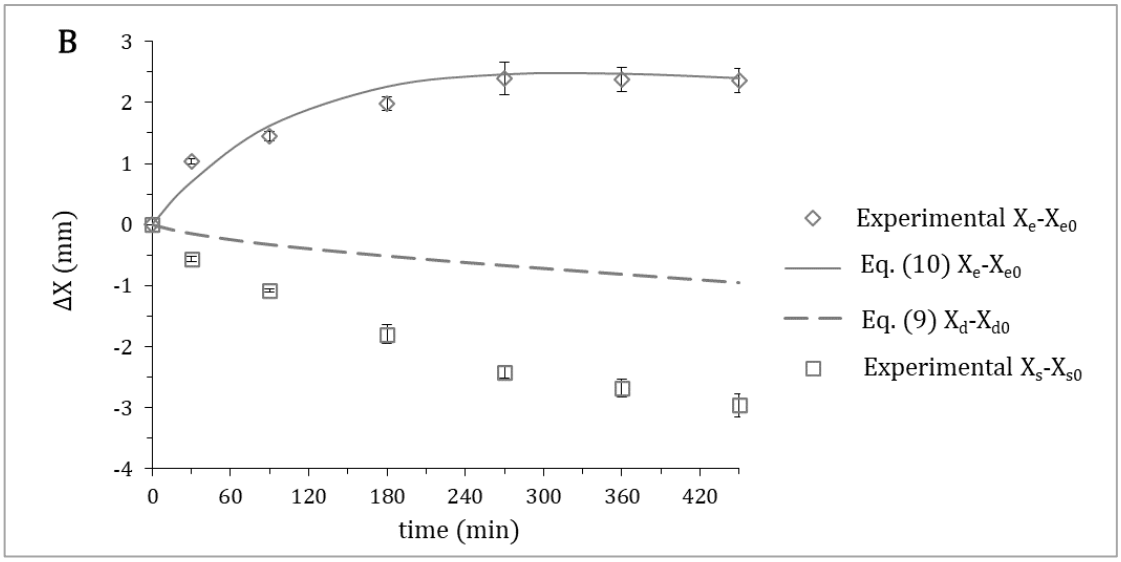

Figure 3. A) Model best fitting (solid line – eq.(5)) to experimental release data (M_d, open circles) of the enzyme-free matrix CM_0. B) Model best fitting (solid line – eq.(10)) to experimental data (open rhombi) referring to the position of the erosion front (X_e) with respect to its initial position (X_{e0}). The dashed line represents the calculated displacement (eq.(9)) of the diffusion front (X_d) from its initial position (X_{d0}). X_s indicates the experimentally detected position (open squares) of the swelling front with respect to its initial position X_{s0}. ΔX represents the distances of the erosion, diffusion and swelling fronts from their original position at t=0. Vertical bars indicate standard deviations (n=3).

The fact that D_m ((6.1 ± 0.32) $\cdot 10^{-9}$ m^2/s) is bigger than acetaminophen diffusivity D in water (7.8 $\cdot 10^{-10}$ m^2/s) simply implies that the gel layer is pervaded by channels in which drug transport occurs not only by diffusion but also by convection (water convective motion inside channels). The high B ((555822 ± 30360) s/m) and the small b ((1.57 ± 0.2) $\cdot 10^{-4}$ s^{-1}) values witness the presence of a thick gel (high B) whose erosion is very slow (low b). In addition, the values of the model fitting parameters allow to predict that the position of the diffusion front (dashed line in Figure 3B – eq.(9)) is always set back from the experimentally detected position of the swelling front (squares), as it is expected.

Model best fitting has also been performed simultaneously on release data and on erosion front position of matrices containing different amount of enzymatic

complex. In Figure 4 results of best fitting model (eq.(5) - solid lines) to release data (symbols) for all the considered formulations are presented.

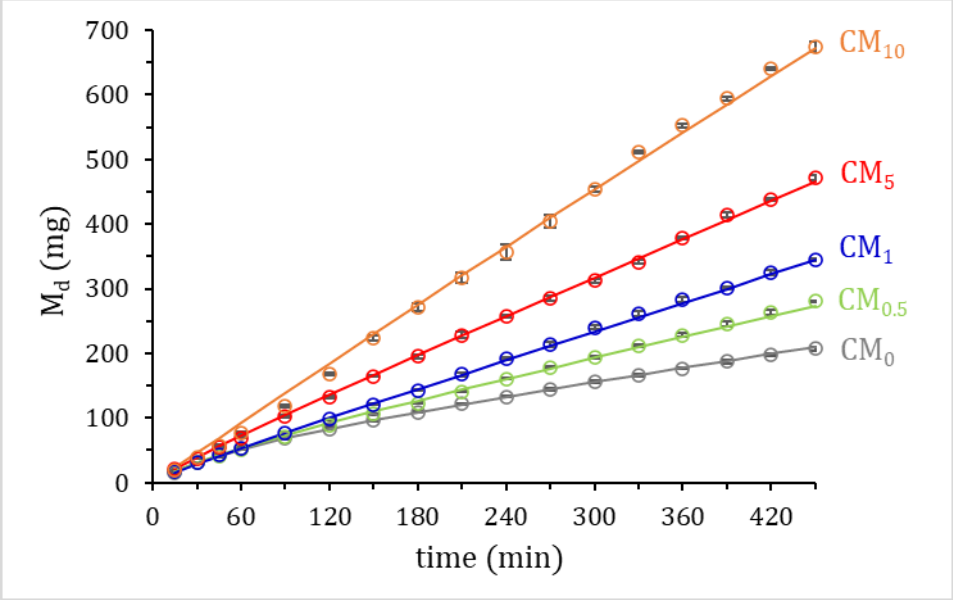

Figure 4. Model best fitting (solid lines – eq.(5)) to experimental release data (M_d, symbols) of partially coated matrices having different cellulase content (CM_0, $CM_{0.5}$, CM_1, CM_5, CM_{10}). Vertical bars indicate standard deviations (n=3).

An excellent agreement has been found between experimental and model best fitting data. This qualitative judgement is statistically supported by the score of the *F*-test reported in Table 3. In addition, model reliability is proved by the physical soundness of the fitting parameters values. Indeed, it can be seen that k_d is almost constant with cellulase content up to 1%, being always lower than that determined by IDR, regardless of the paddle rotation speed. Only when cellulase content is greater or equal to 5%, k_d approaches the intrinsic dissolution rate constant calculated for the lowest rotation speed considered (see Table 2).

Table 3. Model fitting parameters of experimental release data from partially coated matrices with different cellulase content (CM_0, $CM_{0.5}$, CM_1, CM_5, CM_{10}) and score of the statistic F-test for the simultaneous best fitting according to eq.(5) and eq.(9).

Matrix code	$\boldsymbol{CM_0}$	$\boldsymbol{CM_{0.5}}$	$\boldsymbol{CM_1}$	$\boldsymbol{CM_5}$	$\boldsymbol{CM_{10}}$
$F(3,19,0.95)$	< 9660	< 4328	< 21989	< 10266	< 2085
k_d (m/s)	$(4.8 \pm 0.2) \cdot 10^{-6}$	$(4.7 \pm 0.2) \cdot 10^{-6}$	$(4.3 \pm 0.3) \cdot 10^{-6}$	$(5.3 \pm 0.2) \cdot 10^{-6}$	$(5.9 \pm 1.5) \cdot 10^{-6}$
D_m (m^2/s)	$(0.6 \pm 0.32) \cdot 10^{-8}$	$(1.0 \pm 0.05) \cdot 10^{-8}$	$(1.4 \pm 0.21) \cdot 10^{-8}$	$(2.6 \pm 0.20) \cdot 10^{-8}$	$> 10^{-7}$
B (s/m)	555822 ± 30360	285834 ± 14460	131820 ± 14340	75296 ± 8460	< 2000
b $(1/s)$	$(1.6 \pm 0.2) \cdot 10^{-4}$	$(2.8 \pm 0.1) \cdot 10^{-4}$	$(6.2 \pm 1.2) \cdot 10^{-4}$	$(4.3 \pm 0.6) \cdot 10^{-4}$	$> 10^{-3}$

This trend appears justifiable, as in matrices with a high cellulase content, the integrity and uniformity of the gel could be diminished more efficiently. Consequently, this makes the impact of water convection on drug transport no longer negligible. Similarly, considering that the model accounts for the contribution of drug transport by convection, an increase in the diffusion coefficient (Dm) along with the cellulase content suggests an enhanced influence of convection on drug transport within the gel layer.

Finally, the reduction of B and the increase of b with cellulase content point out the formation of a progressively thinner gel layer, that evolves more quickly over time (see eq.(3) and eq.(8)).

The outcomes of model fitting to experimental data can also be depicted by the graph of time evolution of the ratio between drug release resistance due to drug dissolution ($R_d = 1/k_d$) and the total resistance, *i.e.* the sum of R_d and R (resistance due to the formation of the gel layer – eq.(8)) (Figure 5). In all the systems, in the very early stage of drug release ($t \approx 0$ min), the ratio $R_d/(R_d+R)$ is ≈ 1, meaning that the resistance due to the gel layer is almost negligible compared to that due to drug dissolution. As the gel layer thickness - and the associated R- increases, the contribution of Rd to the total resistance progressively diminishes ($0 < t < 120$ min, approximately). This reduction settles at varying values depending on the cellulase content. The lowest plateau value of ($R_d/(R_d + R)$) is observed for CM0 (0.28), and it progressively increases with cellulase concentration to the point that at the highest cellulase concentration, it is maintained close to 1 throughout the whole test period. This trend well correlates with alterations in gel characteristics resulting from cellulase activity, which indeed leads to the formation of a progressively thinner and more permeable swollen layer.

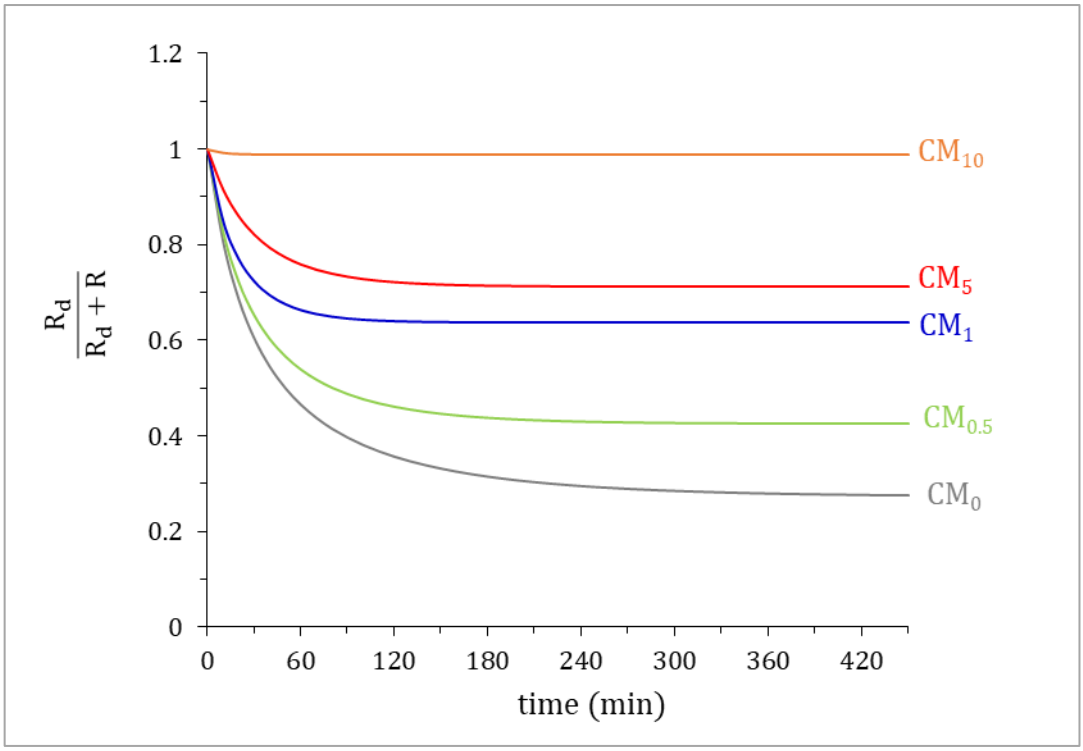

Figure 5. Temporal evolution of the drug dissolution resistance ($R_d = 1/k_d$) with respect to the total resistance (given by R_d and the resistance R exerted by the gel layer, eq.(8)) in partially-coated matrices having different cellulase content (CM_0, $CM_{0.5}$, CM_1, CM_5, CM_{10}).

3.3. Uncoated matrices

Release of drugs from partially coated matrices is, in principle, relatively simpler to describe than from uncoated. In the latter case, drug liberation takes place over the three-dimensional space and the existing fronts are not simple plane surfaces of constant area but consist of complex shape changing over time. Nevertheless, the proposed model proved able to fit the experimental data also in the case of uncoated tablets, as depicted in Figure 6 and supported by the outcome of the F-test reported in Table 4.

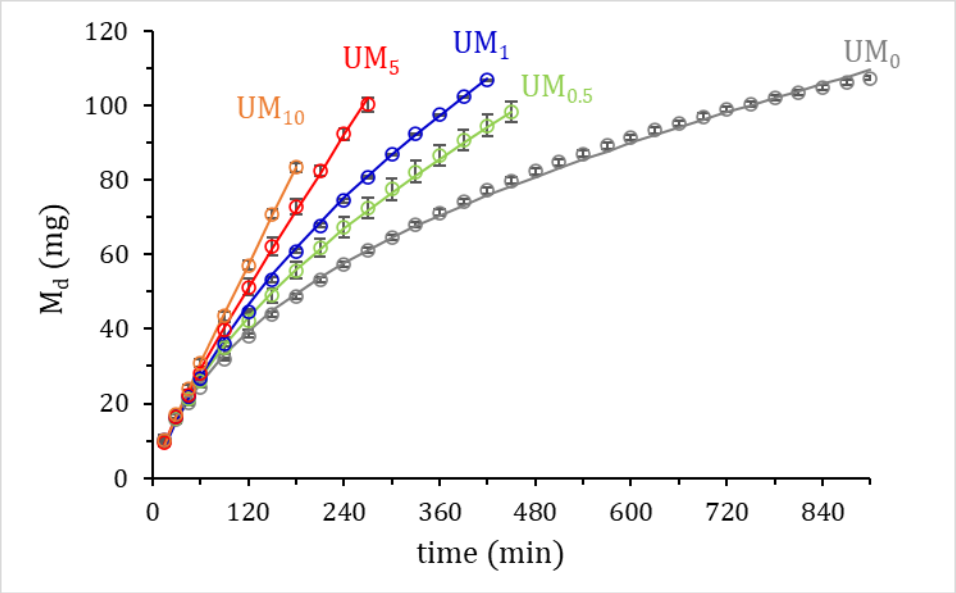

Figure 6. Model best fitting (solid lines – eq.(5)) to experimental release data (M_d, symbols) of uncoated matrices having different cellulase content (UM_0, U$M_{0.5}$, UM_1, UM_5, UM_{10}). Vertical bars indicate data standard deviation (n=3).

Table 4. Model fitting parameters of experimental release data from uncoated matrices with different cellulase content (UM_0, $UM_{0.5}$, UM_1, UM_5, UM_{10}) and score of the statistic F-test for the best fitting according to eq.(5).

Matrix code	$\boldsymbol{UM_0}$	$\boldsymbol{UM_{0.5}}$	$\boldsymbol{UM_1}$	$\boldsymbol{UM_5}$	$\boldsymbol{UM_{10}}$
F-test score	$F(2,29,0.95) < 12700$	$F(2,16,0.95) < 13259$	$F(2,13,0.95) < 10340$	$F(2,8,0.95) < 9078$	$F(2,5,0.95) < 2826$
k_d *(m/s)*	$(4.4\pm0.1) \cdot 10^{-6}$	$(4.3\pm0.2) \cdot 10^{-6}$	$(3.8\pm0.3) \cdot 10^{-6}$	$(4.7\pm0.3) \cdot 10^{-6}$	$(4.3\pm0.7) \cdot 10^{-6}$
B (s/m)	2746066 ± 314340	1019693 ± 14460	1082343 ± 334920	218532 ± 115680	99330 ± 21240
B (1/s)	$(3.1\pm0.5) \cdot 10^{-5}$	$(6.8\pm1.0) \cdot 10^{-5}$	$(3.8\pm1.3) \cdot 10^{-4}$	$(3.6\pm0.6) \cdot 10^{-4}$	$(4.3\pm3.7) \cdot 10^{-4}$

The values of k_d calculated for the uncoated matrices at different cellulase content are rather similar and always lower than those obtained from IDR experiment at any rotational speed (see Table 2). Moreover, k_d values are quite close to those calculated for partially coated tablets (see Table 3), thus substantiating that the dissolution process at the solid-liquid interface is not affected by the different shape of the moving fronts in the two matrix configurations. Temporal evolution of the drug dissolution resistance ($R_d = 1/k_d$) with respect to the total resistance is shown in Figure 7.

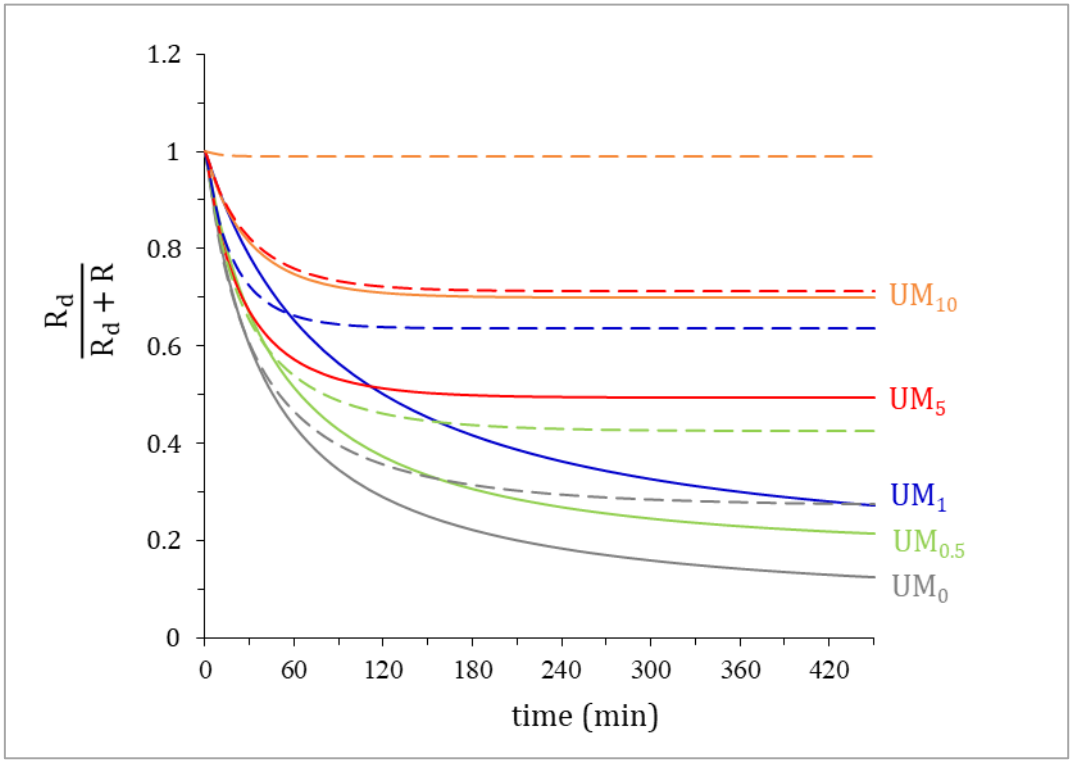

Figure 7. Temporal evolution of the drug dissolution resistance ($R_d = 1/k_d$) with respect to the total resistance (given by R_d and the resistance R exerted by the gel layer, eq.(8)) in uncoated matrices having different cellulase content (UM_0, U$M_{0.5}$, UM_1, UM_5, UM_{10}, coated tablets). Dashed lines represent data of partially-coated matrices having same composition (CM_0, $CM_{0.5}$, CM_1, CM_5, CM_{10}).

Despite an overall similar trend, the uncoated matrices present different kinetics of gel formation and final pseudo-stationary condition as compared to partially

coated ones (dashed line in Figure 7). In fact, whatever the cellulase concentration, the value of $R_d/(R_d + R)$ at the end of the test is always smaller in the case of the uncoated units, which would suggest that the resistance caused by the gel barrier more remarkably affects the release process in the case of uncoated matrices

4. CONCLUSIONS

A mathematical model previously developed was able to describe drug release from HPMC-based HMs containing drugs with different solubility. The applied semi-empirical model took into account the contribution to drug diffusion resistance associated with the dissolution phenomenon and the presence of a gel layer. In the present work, an evaluation of the suitability of such a model to describe drug release from HPMC matrices containing a cellulolytic enzymatic complex (cellulase) was carried out. Preliminary Acetaminophen IDR data obtained at different paddle rotational speed were fitted according to the Levich theory, highlighting good surface wettability properties. The model here reported accurately describes drug release from matrices lacking (free of) and containing increasing amounts of the enzyme.

Two new equations were also introduced that allowed to estimate the position of the erosion and diffusion fronts over time. The experimental data for the position of the erosion front and those predicted by the model were in good agreement, while the diffusion front was found to be consistently positioned between the swelling and erosion fronts.

The output parameters related to gel properties are characterized by physical soundness, according to the expected impact of cellulase. This can be seen by the change in the relative contributions to total resistance associated with both the drug dissolution process and the thickness and permeability of the swollen layer. The enzyme has been shown to progressively reduce gel resistance to drug diffusion over time in a concentration-dependent manner. In fact, for the highest percentage of cellulolytic product, the resulting very thin and permeable gel layer does not contribute at all to the total resistance throughout the whole release test.

The suitability of the proposed equations was also confirmed on uncoated matrices, where the overall picture is complicated by the reduction of the swelling front interface over time.

The dissolution and gel layer contributions to total resistance to drug diffusion as well as fronts positions time course are important aspects to be taken into account for the definition of the release mechanism from HMs. The model successfully described the changes of such phenomena in matrix systems containing an enzyme acting as erosion enhancer. The same equations could be exploited to deepen the possible impact of other “active” excipients on the overall HMs release performance.

References

Abrami, M., Grassi, L., Di Vittorio, R., Hasa, D., Perissutti, B., Voinovich, D., Grassi, G., Colombo, I., Grassi, M., 2020. Dissolution of an ensemble of differently shaped poly-dispersed drug particles undergoing solubility reduction: mathematical modelling. ADMET DMPK 8, 297–313. https://doi.org/10.5599/admet.841

Adrover, A., Varani, G., Paolicelli, P., Petralito, S., Di Muzio, L., Casadei, M.A., Tho, I., 2018. Experimental and Modeling Study of Drug Release from HPMC-Based Erodible Oral Thin Films. Pharmaceutics 10, 222. https://doi.org/10.3390/PHARMACEUTICS10040222

Caccavo, D., Lamberti, G., Barba, A.A., Abrahmsén-Alami, S., Viridén, A., Larsson, A., 2017. Effects of HPMC substituent pattern on water up-take, polymer and drug release: An experimental and modelling study. Int J Pharm 528, 705–713. https://doi.org/10.1016/j.ijpharm.2017.06.064

Caceres, M., Petit, E., Deratani, A., 2020. Partial depolymerization of hydroxypropylmethyl cellulose for production of low molar mass polymer chains. Carbohydr Polym 229, 115461. https://doi.org/10.1016/j.carbpol.2019.115461

Cappello, B., Del Nobile, M.A., La Rotonda, M.I., Mensitieri, G., Miro, A., Nicolais, L., 1994. Water soluble drug delivery systems based on a non-biological bioadhesive polymeric system. Farmaco 49, 809–818.

584 Cerea, M., Foppoli, A., Palugan, L., Melocchi, A., Zema, L., Maroni, A., Gazzaniga,
585 A., 2020a. Non-uniform drug distribution matrix system (NUDDMat) for zero-
586 order release of drugs with different solubility. Int J Pharm 581, 119217.
587 https://doi.org/10.1016/j.ijpharm.2020.119217
588 Cerea, M., Maroni, A., Palugan, L., Bellini, M., Foppoli, A., Melocchi, A., Zema, L.,
589 Gazzaniga, A., 2018. Novel hydrophilic matrix system with non-uniform drug
590 distribution for zero-order release kinetics. Journal of Controlled Release 287,
591 247–256. https://doi.org/10.1016/j.jconrel.2018.08.027
592 Cerea, M., Maroni, A., Palugan, L., Moutaharrik, S., Melocchi, A., Zema, L., Foppoli,
593 A., Gazzaniga, A., 2020b. Oral hydrophilic matrices having non uniform drug
594 distribution for zero-order release: A literature review. Journal of Controlled
595 Release 325, 72–83. https://doi.org/10.1016/j.jconrel.2020.06.033
596 Chirico, S., Dalmoro, A., Lamberti, G., Russo, G., Titomanlio, G., 2007. Analysis and
597 modeling of swelling and erosion behavior for pure HPMC tablet. Journal of
598 Controlled Release 122, 181–188.
599 https://doi.org/10.1016/j.jconrel.2007.07.001
600 Colombo, P., 1993. Swelling-controlled release in hydrogel matrices for oral route.
601 Adv Drug Deliv Rev 11, 37–57. https://doi.org/10.1016/0169-
602 409X(93)90026-Z
603 Colombo, P., Bettini, R., Massimo, G., Catellani, P.L., Santi, P., Peppas, N.A., 1995.
604 Drug diffusion front movement is important in drug release control from
605 swellable matrix tablets. J Pharm Sci 84, 991–997.
606 Colombo, P., Bettini, R., Peppas, N.A., 1999. Observation of swelling process and
607 diffusion front position during swelling in hydroxypropyl methyl cellulose
608 (HPMC) matrices containing a soluble drug. Journal of Controlled Release 61,
609 83–91.
610 Colombo, P., Bettini, R., Santi, P., Peppas, N.A., 2000. Swellable matrices for
611 controlled drug delivery: gel-layer behaviour, mechanisms and optimal
612 performance. Pharm Sci Technol Today 3, 198–204.
613 https://doi.org/10.1016/S1461-5347(00)00269-8
614 Colombo, P., Gazzaniga, A., Caramella, C., Conte, U., La Manna, A., 1987. In vitro
615 programmable zero-order release drug delivery system. Acta Pharmaceutica
616 Technologica 33, 15–20.

Conte, U., Maggi, L., Colombo, P., Manna, A. La, 1993. Multi-layered hydrophilic matrices as constant release devices (GeomatrixTM Systems). Journal of Controlled Release 26, 39–47.

Deering, R.P., Kommareddy, S., Ulmer, J.B., Brito, L.A., Geall, A.J., 2008. Modulation of drug release from hydrophilic matrices. Pharmaceutical Technology Europe 20, 885–899. https://doi.org/10.1517/17425247.2014.901308

Demidovic, B.P., 1975. Esercizi e problemi di analisi matematica, Sixth. ed. Editori Riuniti, Rome.

ECHA, 2012. Paracetamol Registration Dossier [WWW Document]. URL https://echa.europa.eu/it/registration-dossier/-/registered-dossier/12532/4/5 (accessed 11.7.23).

Ferrero, C., Massuelle, D., Doelker, E., 2010. Towards elucidation of the drug release mechanism from compressed hydrophilic matrices made of cellulose ethers. II. Evaluation of a possible swelling-controlled drug release mechanism using dimensionless analysis. Journal of Controlled Release 141, 223–233. https://doi.org/10.1016/j.jconrel.2009.09.011

Flynn, G.L., Yalkowskyx, S.H., Roseman, T.J., 1974. Mass Transport Phenomena and Models: Theoretical Concepts. J Pharm Sci 63, 479–510.

Foppoli, A., Maroni, A., Palugan, L., Zema, L., Moutaharrik, S., Melocchi, A., Cerea, M., Gazzaniga, A., 2020. Erodible coatings based on HPMC and cellulase for oral time-controlled release of drugs. Int J Pharm 585, 119425. https://doi.org/10.1016/j.ijpharm.2020.119425

Ford, J.L., Rubinstein, M.H., McCaul, F., Hogan, J.E., Penny Edgar, -and J, 1987. Importance of drug type, tablet shape and added diluents on drug release kinetics from hydroxypropylmethylcellulose matrix tablets. Int J Pharm 40, 223–234.

Gander, B., Gurny, R., Doelker, E., Peppas, N.A., 1988. Crosslinked Poly(Alkylene Oxides) for the preparation of controlled release micromatrices. Journal of Controlled Release 5, 271–283.

Gazzaniga, A., Moutaharrik, S., Filippin, I., Foppoli, A., Palugan, L., Maroni, A., Cerea, M., 2022. Time-Based Formulation Strategies for Colon Drug Delivery. Pharmaceutics 14, 2762. https://doi.org/10.3390/pharmaceutics14122762

650 Gazzaniga, A., Sangalli, M.E., Conte, U., Caramella, C., Colombo, P., La Manna, A.,
651 1993. On the release mechanism from coated swellable minimatrices. Int J
652 Pharm 91, 167–171. https://doi.org/10.1016/0378-5173(93)90336-E
653 Ghori, M.U., Conway, B.R., 2015. Hydrophilic Matrices for Oral Control Drug
654 Delivery. Am J Pharmacol Sci 3, 103–109.
655 https://doi.org/https://doi.org/10.12691/ajps-3-5-1
656 Grassi, M., Grassi, G., Lapasin, R., Colombo, I., 2006. Drug Dissolution and
657 Partitioning, in: Understanding Drug Release and Absorption Mechanisms. A
658 Physical and Mathematical Approach. CRC Press, Boca Raton, FL, pp. 249–
659 332. https://doi.org/10.1201/9781420004656
660 Grassi, M., Zema, L., Sangalli, M.E., Maroni, A., Giordano, F., Gazzaniga, A., 2004.
661 Modeling of drug release from partially coated matrices made of a high
662 viscosity HPMC. Int J Pharm 276, 107–114.
663 https://doi.org/10.1016/j.ijpharm.2004.02.016
664 Guiastrennec, B., Söderlind, E., Richardson, S., Peric, A., Bergstrand, M., 2017. In
665 Vitro and In Vivo Modeling of Hydroxypropyl Methylcellulose (HPMC) Matrix
666 Tablet Erosion Under Fasting and Postprandial Status. Pharm Res 34, 847–
667 859. https://doi.org/10.1007/s11095-017-2113-7
668 Harland, R.S., Gazzaniga, A., Sangalli, M.E., Colombo, P., Peppas, N.A., 1988.
669 Drug/Polymer Matrix Swelling and Dissolution. Pharmaceutical Research: An
670 Official Journal of the American Association of Pharmaceutical Scientists 5,
671 488–494. https://doi.org/10.1023/A:1015913207052
672 Iqbal, M.J., Malik, Q.M., 2005. Partial molar volume of paracetamol in water, 0.1M
673 HCl and 0.154M NaCl at T=(298.15, 303.15, 308.15 and 310.65)K and at
674 101.325kPa. J Chem Thermodyn 37, 1347–1350.
675 https://doi.org/10.1016/j.jct.2005.03.008
676 Jamzad, S., Tutunji, L., Fassihi, R., 2005. Analysis of macromolecular changes and
677 drug release from hydrophilic matrix systems. Int J Pharm 292, 75–85.
678 https://doi.org/10.1016/j.ijpharm.2004.11.011
679 Jantzen, G.M., Robinson, J.R., 2002. Sustained- and Controlled-Release Drug
680 Delivery Systems, in: Banker, G., Rhodes, C. (Eds.), Modern Pharmaceutics.
681 Marcel Dekker, Basel, pp. 503–530.

Khoury, N., Mauger, J.W., Howard, S., 1988. Dissolution Rate Studies from a Stationary Disk/Rotating Fluid System. Pharm Res 5, 495–500.

Kim, C. ju, 1995. Compressed Donut-Shaped Tablets with Zero-Order Release Kinetics. Pharmaceutical Research: An Official Journal of the American Association of Pharmaceutical Scientists 12, 1045–1048. https://doi.org/10.1023/A:1016218716951

Laracuente, M.L., Yu, M.H., McHugh, K.J., 2020. Zero-order drug delivery: State of the art and future prospects. Journal of Controlled Release 327, 834–856. https://doi.org/10.1016/j.jconrel.2020.09.020

Levich, V.G., 1962. Physicochemical Hydrodynamics. Prentice-Hall, Englewood, NJ.

Lombardi, C., Zema, L., Sangalli, M.E., Maroni, A., Giordano, F., Gazzaniga, A., 1998. Influence of drug/polymer ratio on the release from heterogeneous high viscosity HPMC matrices. ., in: World Meeting APGI/APV. pp. 335–336.

Loreti, G., Maroni, A., Dorly, M., Curto, D., Melocchi, A., Gazzaniga, A., Zema, L., 2013. Evaluation of hot-melt extrusion technique in the preparation of HPC matrices for prolonged release. https://doi.org/10.1016/j.ejps.2013.10.014

Mašková, E., Kubová, K., Raimi-Abraham, B.T., Vllasaliu, D., Vohlídalová, E., Turánek, J., Mašek, J., 2020. Hypromellose-A traditional pharmaceutical excipient with modern applications in oral and oromucosal drug delivery. Journal of Controlled Release 324, 695–727. https://doi.org/10.1016/j.jconrel.2020.05.045

Moodley, K., Pillay, V., Choonara, Y.E., du Toit, L.C., Ndesendo, V.M.K., Kumar, P., Cooppan, S., Bawa, P., 2011. Oral Drug Delivery Systems Comprising Altered Geometric Configurations for Controlled Drug Delivery. Int J Mol Sci 13, 18–43. https://doi.org/10.3390/ijms13010018

Palugan, L., Filippin, I., Cirilli, M., Moutaharrik, S., Zema, L., Cerea, M., Maroni, A., Foppoli, A., Gazzaniga, A., 2021. Cellulase as an “active” excipient in prolonged-release HPMC matrices: A novel strategy towards zero-order release kinetics. Int J Pharm 607, 121005. https://doi.org/10.1016/j.ijpharm.2021.121005

Peppas, N.A., Narasimhan, B., 2014. Mathematical models in drug delivery: How modeling has shaped the way we design new drug delivery systems. Journal

715 of Controlled Release 190, 75–81.
716 https://doi.org/10.1016/j.jconrel.2014.06.041
717 Ranga Rao, K V, Padmalatha Devi, K., Buri, P., Ranga Rao, KV, 1988. Cellulose
718 Matrices for Zero-Order Release of Soluble Drugs. Drug Dev Ind Pharm 14,
719 2299–2320. https://doi.org/10.3109/03639048809152017
720 Rogers T L, 2009. Hypromellose, in: Rowe, R.C., Sheskey, P.J., Quinn, M.E. (Eds.),
721 Handbook of Pharmaceutical Excipients. Pharmaceutical Press, London, pp.
722 326–329.
723 Saeidipour, F., Mansourpour, Z., Mortazavian, E., Rafiee-Tehrani, N., Rafiee-
724 Tehrani, M., 2017. New comprehensive mathematical model for HPMC-MCC
725 based matrices to design oral controlled release systems. European Journal of
726 Pharmaceutics and Biopharmaceutics 121, 61–72.
727 https://doi.org/10.1016/j.ejpb.2017.09.007
728 Sai Cheong Wan, L., Wan Sia Heng, P., Fun Wong, L., 1995. Matrix swelling: A
729 simple model describing extent of swelling of HPMC matrices. Int J Pharm
730 116, 159–168. https://doi.org/10.1016/0378-5173(94)00285-D
731 Salsa, T., Veiga, F., Pina, M.E., 2008. Oral Controlled-Release Dosage Forms. I.
732 Cellulose Ether Polymers in Hydrophilic Matrices. Drug Dev Ind Pharm 23,
733 929–938. https://doi.org/10.3109/03639049709148697
734 Sangalli, M.E., Giunchedi, P., Maggi, L., Conte, U., Gazzaniga, A., 1994. Inert
735 monolithic device with a central hole for constant drug release. European
736 Journal of Pharmaceutics and Biopharmaceutics 40, 370–373.
737 Siepmann, J., Peppas, N.A., 2012. Modeling of drug release from delivery systems
738 based on hydroxypropyl methylcellulose (HPMC). Adv Drug Deliv Rev 64,
739 163–174. https://doi.org/10.1016/j.addr.2012.09.028
740 Siepmann, J., Peppas, N.A., 2001. Modeling of drug release from delivery systems
741 based on hydroxypropyl methylcellulose (HPMC). Adv Drug Deliv Rev 48,
742 139–157. https://doi.org/10.1016/S0169-409X(01)00112-0
743 Timmins, P., Desai, D., Chen, W., Wray, P., Brown, J., Hanley, S., 2016. Advances
744 in mechanistic understanding of release rate control mechanisms of extended-
745 release hydrophilic matrix tablets. Ther Deliv 7, 553–572.
746 https://doi.org/10.4155/tde-2016-0026

747 Tiwari, S.B., Rajabi-Siahboomi, A.R., 2008. Extended-Release Oral Drug Delivery
748 Technologies: Monolithic Matrix Systems, in: Jain, K.K. (Ed.), Drug Delivery
749 Systems. Humana Press, Totowa, NJ, pp. 217–244.
750 Tiwari, S.P., DiNunzio, J., Rajabi-Siahboomi, A., 2011. Drug–Polymer Matrices for
751 Extended Release, in: Wilson, C.G., Crowley, P.J. (Eds.), Controlled Release in
752 Oral Drug Delivery. Springer, New York, pp. 131–159.
753 Vázquez, M.J., Pérez-Marcos, B., Gómez-Amoza, J., Martinez -Pacheco, R., Souto,
754 C., Concheiro, A., 1992. Influence of technological variables on release of
755 drugs from hydrophilic matrices. Drug Dev Ind Pharm 18, 1355–1375.
756 https://doi.org/10.3109/03639049209046332
757 Wang, S., Liu, R., Fu, Y., Kao, W.J., 2020. Release mechanisms and applications of
758 drug delivery systems for extended-release. Expert Opin Drug Deliv 17, 1289–
759 1304. https://doi.org/10.1080/17425247.2020.1788541
760 Wen, X., Nokhodchi, A., Rajabi-Siahboomi, A., 2010. Oral extended release
761 hydrophilic matrices: formulation and design, in: Wen, H., Park, K. (Eds.), Oral
762 Controlled Release Formulation Design and Drug Delivery : Theory to
763 Practice. Wiley, New Jersey, pp. 89–100.
764 Zhang, F., McGinity, J.W., 1999. Properties of Sustained-Release Tablets Prepared
765 by Hot-Melt Extrusion. Pharm Dev Technol 4, 241–250.
766 https://doi.org/10.1081/PDT-100101358
767